

Article

Improving the Quality of Laser-Welded Butt Joints of Metal–Polymer Sandwich Composites

Serguei P. Murzin ^{1,2,*} , Heinz Palkowski ^{2,3} , Alexey A. Melnikov ², Maksim V. Blokhin ² and Stanislav Osipov ¹¹ TU Wien, Karlsplatz 13, 1040 Vienna, Austria; stanislav.osipov@tuwien.ac.at² Samara National Research University, Moskovskoe Shosse 34, 443086 Samara, Russia;

heinz.palkowski@tu-clausthal.de (H.P.); melnickov.alex@yandex.ru (A.A.M.); m.v.blokhin@yandex.ru (M.V.B.)

³ Institute of Metallurgy (IMET), Clausthal University of Technology, 38678 Clausthal-Zellerfeld, Germany

* Correspondence: murzin@ssau.ru or serguei.murzin@tuwien.ac.at

Abstract: Sandwich panels are promising composite materials, although the possibilities for their thermal joining are limited due to the degradation of the polymer core at elevated temperatures. The purpose of this study is to improve the quality of the butt joints in metal–polymer sandwich composites performed by laser welding. A pulsed Nd:YAG Rofin StarWeld Performance laser was used to perform the two-sided welding of the metal–polymer three-layer composite material. On each of the two sides of the material, a welded joint was made with partial penetration of the covering steel sheets, which was considered a prerequisite for preventing the degradation of the core polymer layer. The energy density of the laser irradiation was redistributed by increasing the diameter of the laser spot. The structure of the welded joints was examined using a polarized optical microscope and a scanning electron microscope. It was determined that the laser treatment resulted in a partial penetration weld on each of the two covering metal sheets of the material, reaching a depth of more than 50% of the sheet's thickness without damaging the polymer. The welding area consisted of two zones, one being the weld metal and the other the heat-affected zone. As a result of relatively rapid heating and cooling cycles, fine-dispersed structures were formed in the heat-affected and remelted zones. The performed tensile tests showed that the strength of the welded area was about 80% of that of the base material.

Keywords: metal–polymer; sandwich composites; laser welding; butt joint; partial penetration; microstructure



Citation: Murzin, S.P.; Palkowski, H.; Melnikov, A.A.; Blokhin, M.V.; Osipov, S. Improving the Quality of Laser-Welded Butt Joints of Metal–Polymer Sandwich Composites. *Appl. Sci.* **2022**, *12*, 7099. <https://doi.org/10.3390/app12147099>

Academic Editor: Jean-Pierre Bergmann

Received: 21 June 2022

Accepted: 12 July 2022

Published: 14 July 2022

Publisher's Note: MDPI stays neutral with regard to jurisdictional claims in published maps and institutional affiliations.



Copyright: © 2022 by the authors. Licensee MDPI, Basel, Switzerland. This article is an open access article distributed under the terms and conditions of the Creative Commons Attribution (CC BY) license (<https://creativecommons.org/licenses/by/4.0/>).

1. Introduction

Sandwich panels are promising composite materials, combining the advantages that mono-materials often cannot offer, such as high bending resistance, good energy absorption, as well as high load-carrying capacity combined with low specific weight [1–3]. However, the possibilities for thermal joining for producing long-length tailor-made multilayer composite components based on polymers, e.g., for the automotive industry, are limited due to the instability of the polymer core at elevated temperatures. The degradation of the polymer during the welding of cover metal sheets leads not only to corrosive effects that should be avoided [4]. High temperature can negatively affect the properties of the central layer and lead to a significant local deterioration in the damping and acoustic properties of the sandwich material. In Refs. [5,6], laser welding was proposed as a technique for accomplishing the task of joining such parts. A two-sided welding scheme, whereby the sandwich material must be welded on both sides to completely eliminate or significantly reduce the thermal impact on the polymer core, was recommended in [7,8]. However, these Refs. [5–8] describe the results of one-sided welding only, whereby it was not possible to obtain a weld without completely removing the polymer layer. Considering the results of these studies, it was reported in [9] that laser welding cannot be applied to multilayer materials without damaging the central polymer layer.

One of the first successful two-sided welding procedures was achieved in [10]. It was determined that two-sided pulsed-periodic laser welding could be accomplished for each of the two metal layers without significant degradation of the middle polymer layer using specific treatment parameters. A thermal cycle with high heating and cooling rates ensured a significant reduction in the heat-affected zone during laser welding. It was established that the reduced volume of molten metal and the specific shape of the weld can influence the crystallization conditions, which, in turn, will provide an opportunity to increase the technological strength and mechanical properties of the welded joints. Only a limited weld depth and a relatively low strength during tensile tests, associated as well with the relatively small cross-sectional area, were achieved. Therefore, improving the quality of the welded joint was considered to be the main prospective research objective. It was assumed that the structure of the welded joint can be improved by redistributing the power density and energy of the laser beam.

There are various possibilities for improving the quality and strength of a laser-welded joint. The influence of power distribution of a continuous-wave laser on the weld quality and geometry, including the welded joint microstructure, the penetration depth, the weld width and porosity, were investigated in [11–16]. It was demonstrated that one of the methods for obtaining a relatively wide weld with lower requirements for edge alignment is welding using a defocused beam [17,18]. When using a pulsed-periodic beam, the redistribution of energy density can also provide an opportunity to improve the structure and properties of the welded joint. For example, in [19,20], a method was studied where overlap conduction mode welding was used to produce a shaped joint of sheet materials. In this case, it was possible to adjust the penetration depth by changing the pulse energy and duration.

In [21], the authors investigated the influence of the process parameters on the quality and strength of the welded joint during pulse-periodic butt welding of 1.5 mm thick stainless-steel sheets. The most important parameters that were evaluated were the angle of incidence of the laser beam, the laser power and the welding speed. Although during welding, the energy redistribution took place by varying the angle of incidence, the effect of this parameter was not investigated separately. It was noted in [22] that the reduction in the peak power in the pulse with increasing spot diameter reduces the peak power density, thus, reducing the penetration depth. There are maximum and minimum values for both the spot diameter and peak power. It was demonstrated that the small spot diameter and, therefore, high power densities not only contribute to increased depth of the welding zone, but also to the formation of spatter on the surfaces to be welded.

In [23], along with such technological factors as laser beam power, welding speed, overlap factor, pulse duration and shape, the effect of laser spot diameter on the quality of pulsed butt welding of dual-phase steel was investigated. It was determined that during constant energy and pulse duration, an effect of reduction in penetration takes place when the spot diameter increases over the critical value, at which the spattering of metallic material stops. It was also established that the remelted zone of the butt joint was harder than both the base metal and the metal within the heat-affected zone, which was not subjected to melting.

In [24], the results of pulsed laser butt welding of nickel-based superalloy samples are presented. The possibility of improving the quality of the welded joint by redistributing the energy density of laser irradiation with increasing the size of the laser spot was demonstrated. The assessment of strength properties of joints proved this statement. In [25], it was determined that laser exposure with its well-defined and accurately localized energy input offers the possibility to reduce the growth of intermetallic layers in the butt joint. The necessity of using special optics for a more precise dosage and the ability to perform a special redistribution of the laser beam energy locally in the laser treatment area was determined. As a rule, hardening structures with low plasticity and developed interdendritic microheterogeneity, which are characterized by increased hardness, are formed in the cast zone. When the size of the impacting laser spot is increased, the cooling rate decreases

slightly. This can eliminate the possibility of the formation of a coarse-grained dendritic structure, which is prone to brittle fracture.

The purpose of this study is to improve the quality of the butt joint of metal–polymer sandwich composites during laser welding by redistributing the energy density of laser irradiation while increasing the diameter of the laser spot. It should be noted that increasing the diameter of the laser spot requires an increase in the total energy, which is supplied to the material. During the welding of metal–polymer composites, this can have a negative impact on the polymer core. To avoid this problem, partial penetration of the steel sheets was adopted as a prerequisite to avoid degradation of the polymer core layer.

2. Experimental Equipment

The welding of the metal–polymer three-layer composite material was performed using a pulsed Nd:YAG Rofin StarWeld Performance laser (Rofin-Baasel Lasertech GmbH & Co. KG, Headquarters Laser Micro, Gilching, Germany) in a basic configuration, equipped with a Sweet Spot resonator for welding materials that are sensitive to changes of laser parameters. This mobile unit is equipped with a laser having a wavelength of 1.06 μm providing a nominal output power of 50 W and having a system of motorized laser spot expansion in a working plane in a range from 0.25 to 2 mm. The maximal achievable parameters are the pulse energy of 100 J and the peak power of 9 kW, while the pulse duration can be varied between 0.5 and 50 ms, at a frequency of a single pulse in the range of 0.5–50 Hz. The laser system is also equipped with an internal water-IR heat exchanger cooling unit and a connection for shielding gas and cooling air. The main processing operations of parts using the pulse shaping system were performed in the working chamber, which is equipped with fixed and flexible nozzles through which cooling and shielding gas (e.g., argon) can be supplied. An exhaust unit with filter is integrated in the working chamber, which ensures a 99.997% degree of air purification. A Leica microscope offers the possibility to magnify the viewing area by 24-times during material welding and 2.5D motorized device is a part of the CNC control module. The maximum traverse speed is 10 mm/s, with a linear displacement resolution of 2.5 μm and a positioning accuracy of less than 20 μm , resulting in a high-quality welded joint.

A VEGA\SB, Tescan (Tescan, a.s., Brno, Czech Republic) analytical scanning electron microscope (SEM) with a tungsten thermal emission cathode as an electron source was used to examine the welded joints obtained by pulse-periodic laser exposure. The microscope is equipped with two integrated detectors: an Everhart-Thornley type secondary electron detector (SE) for imaging with topographical contrast and a back-scattered electron detector (BSE) for imaging with compositional contrast, which allows one to record both the surface morphology and the local elemental composition of the sample. The range of electron beam energy is between 200 eV and 30 keV. An electromagnetic lens is used as a device for changing apertures to adjust the beam current. The magnification is continuous in a range from 2 to 10^6 -times. Electron microscope resolution in high-vacuum mode is 3 nm at 30 keV using an SE detector. Polarization-optical microscope Neophot-30 (Carl Zeiss Jena GmbH, Jena, Germany) with magnification range of 10–2000-times was used for metallographic investigation of the sample surface structure. The principle of its operation is based on the analysis of light reflected from the surface.

The Shimadzu AGS-100kNX testing machine (Shimadzu Europa GmbH, Duisburg, Germany) with a maximum measured force of 100 kN was used to perform tensile tests in order to evaluate the mechanical properties of the welded joint. This represents an electro-mechanical testing system performing a direct high-precision loading method and using a precision drive with a screw on a ball bearing with constant control of the deformation of the material under study.

3. Results and Discussion

The two-sided welding was carried out for steel–polymer three-layered composite samples made from DPK 30/50+ZE 0.48 mm thick, dual-phase (DP) steel sheets (HCT500X, 1.0939 [26], ThyssenKrupp Steel Europe AG, Duisburg, Germany). The steel sheets were subjected to electrolytic galvanizing. A 0.6 mm thick thermoplastic polyolefin (polypropylene-polyethylene—PP/PE, Konrad Hornschuh AG, Weißbach, Germany) foil was used as core material [27,28]. These three-layered samples are abbreviated further on “MPM”. Two-sided welding of a three-layer composite material with a partial penetration of each covering steel layer on two sides of the material was carried out.

The surface condition of the joint to be welded largely determines the quality of laser welding. The surface was cleaned from impurities and degreased with the acetone organic solvent. The area to be welded was prepared by mechanical machining. Even small bumps, dents and scratch marks after edge cutting, which is usually carried out after all mechanical preparation operations of samples, have a negative effect on the weld quality, contributing to the formation of hot cracks. To avoid such defects, the preparation of the samples for welding was performed by machining the edges. As the external surfaces of the samples were electrolytically galvanized, it was necessary to remove the zinc coating by grinding the surface in the area of the welded joint foreseen.

The quality and reliability of laser-welded joints also depend on the accuracy of the assembling of the elements to be welded. This assembly must ensure that the edges are close together over the entire length of the weld, with a minimal gap and edge misalignment. The offset of one edge in relation to the other must not exceed a certain value from the thickness of the parts to be welded. The non-rectilinearity of the surfaces to be welded was maintained below 0.03 mm over the entire weld length. In order to eliminate the need for the so-called slope up, i.e., controlled increase in the beam power at the beginning of the welding, and slope down—controlled decrease in the beam power at the end of the welding—entry and exit strips were used. These were clamped to the specimen to obtain a good thermal contact during welding and after the joint was made, the strips were removed.

The criterion for the welding quality is the strength of the joint, which is directly related to the size of the welded area. If the pulse energy is increased, then the depth and diameter of the weld penetration zone increase. It is assumed that the strength of the joint should increase. When reaching a particular value of energy, the power density becomes sufficient for ejecting a portion of the molten metal from the welding pool due to intense evaporation. In this case, the cross-sectional area of the molten zone is reduced; simultaneously, the strength of the joint decreases. For the investigated samples at a pulse duration of 1–3 ms and less, a relatively small cross-sectional area of the molten zone is explained by a relatively small penetration depth as a consequence of reaching intense evaporation early and ejection of the molten metal from the weld pool due to high power density. For example, as shown in Figure 1, at a pulse duration of 1 ms for a spot diameter of 0.45 mm, the maximum penetration depth does not exceed 0.16 mm. When the pulse duration is increased, the ultimate depth and diameter of the molten zone increases. However, the portion of the energy lost through heat dissipation due to thermal conduction increases. Therefore, the overall energy required to start the melting of the metal increases. At a pulse duration greater than 20–30 ms, a further increase in duration no longer results in an even greater increase in the size of the molten zone due to an increase in the energy loss by thermal conduction for the samples under investigation.

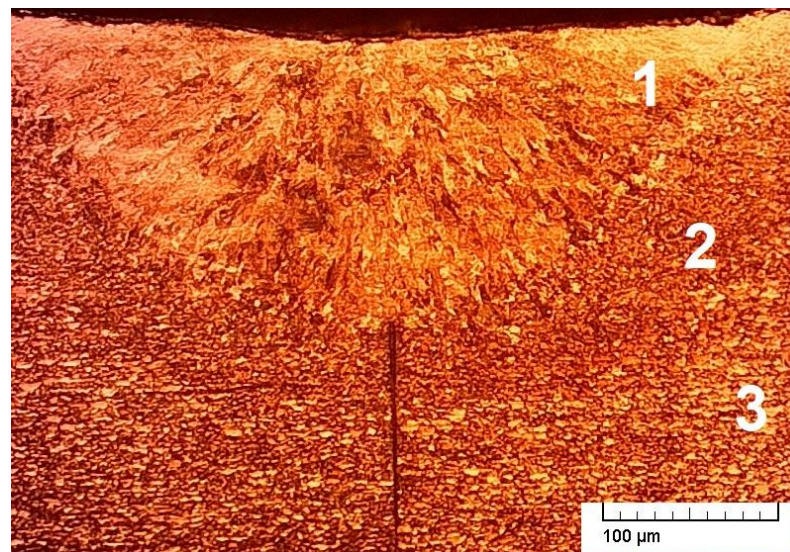


Figure 1. Typical cross-section of the laser butt welding zone of the upper layer of a steel–polymer three-layer composite sample at a pulse duration of 1 ms: 1—remelted zone with a developed interdendrite microheterogeneity; 2—heat-affected zone; 3—initial metal.

Once the optimum laser spot diameter was achieved, a further increase in its size caused a decrease in temperature on the material surface and, consequently, a decrease in penetration depth. It was determined that energy control for laser welding in the conduction mode by keeping the surface conditions just below the material evaporation point allows one to achieve maximum penetration. Material melting, in this case, is a sufficiently stable process and there is a real possibility of obtaining high-quality welds without pore formation and spattering of the material. Suitable regimes for laser welding of steels must provide a combination of such parameters as qualitative weld formation, sufficient operating strength and acceptable mechanical properties in the welded joint. A necessary pre-requisite for the absence of degradation of the core polymer layer will be a partial penetration weld, i.e., a weld in which the fusion penetration is intentionally less than full penetration of the external metal layer.

For regimes with significant evaporation, a more intense formation of pores and discontinuities was observed; therefore, conduction welding was carried out in such cases where the heat generation density was not high enough to cause intensive evaporation of the material. The results of experimental studies demonstrated that, for specific values of energy and pulse duration, there is a certain diameter of the laser spot at which fusion penetration reaches a maximum. By gradually increasing the diameter of the laser spot, an increase in penetration depth was observed only until evaporation of the material ceased, i.e., when the surface temperature became equal to the evaporation temperature.

The parameters of the pulsed-periodic laser welding were determined. The laser pulse configuration was chosen with an extended pulse leading edge. Laser welding with pulse energy of 32 J at a pulse duration of 8 ms and a pulse frequency of 1 Hz, at which the size of the laser spot on the material surface was 0.75 mm, provided satisfactory results. The optical system had a focal distance of 7.5 inches and the focal plane was above the material surface. Figure 2 shows the top view of the joint created by welding metal–polymer samples made of MPM alternately on both sides.

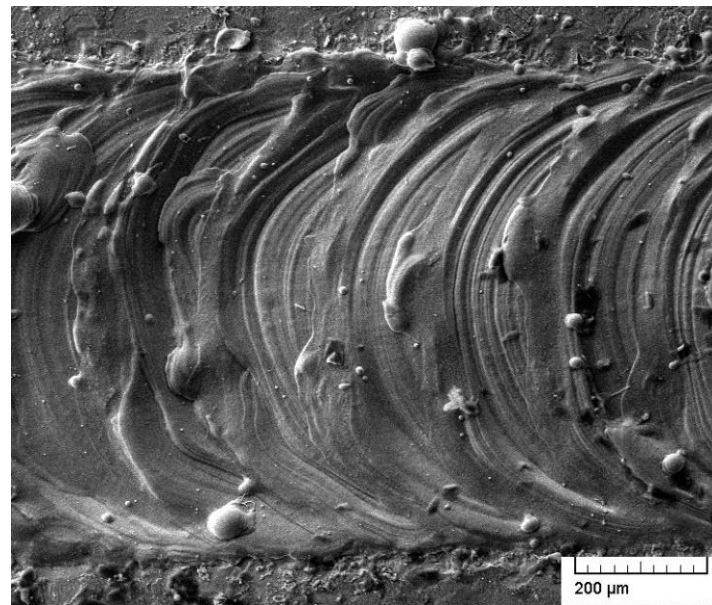


Figure 2. Top view of the welded joint.

The structure of the laser-butt-welded joints was examined on prepared samples after welding. The surface of the prepared microsections was chemically etched. The samples were examined visually and using a Neophot-30 microscope. In order to enhance the contrast in the image of the microstructure, an oblique illumination was used. Figure 3 shows the etched microsection of the welded joint in the MPM. As can be seen, the weld was performed only to the half of the thickness of each covering steel sheet. Figure 4 shows a microsection of the welded joint in the top layer of an MPM sample. The welding area consists of two zones, one being the weld metal and the other the heat-affected zone that is a part of the unmolten original metal, the microstructure of which was affected. The weld metal does not contain a coarse-grained cast structure. Microscopic cavities with external inclusions, as well as very small, single gas pores were also identified during investigation. Other weld defects were not detected in the examined samples.

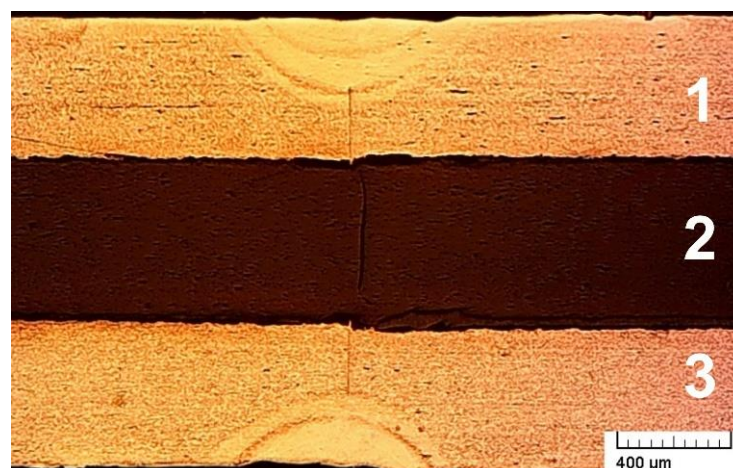


Figure 3. Cross-section of the joint area: 1, 3—dual-phase steel sheets with a thickness of 0.48 mm; 2—the core material with a thickness of 0.6 mm.

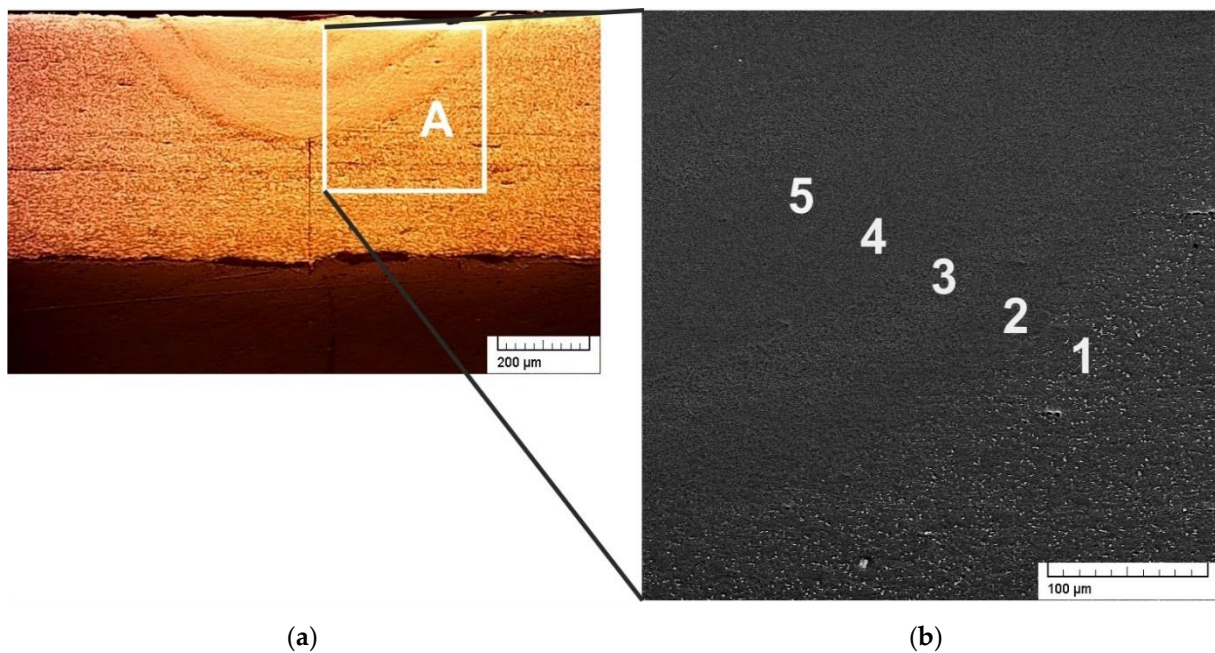


Figure 4. (a) Microsection of the welded joint in the upper layer of the MPM sample, registered using a Neophot-30 microscope. To enhance the contrast in the surface image of the microstructure an oblique illumination was used; (b) cross-section of part A of the heat-affected zone recorded using a VEGA\SB, Tescan SEM: 1—the base metal; 2, 3—the heat-affected zone; 4, 5—the welded metal.

The morphology of the laser-welded zones of covering sheets made of 1.0939/HCT500X steel was examined with a VEGA\SB, Tescan SEM. It is known that the initial microstructure of the material (region 1 in Figure 4) consists of elongated grains with an average size of about 5 μm . These grains are stretched in the rolling direction and form a characteristic ferrite–martensite structure. As shown in Figure 5, martensite islands are dispersed in a soft ferrite matrix, resulting in medium strength at sufficient steel impact toughness. The ferrite phase with lower strength is usually continuous, which imparts the ductility required for various applications to this steel.

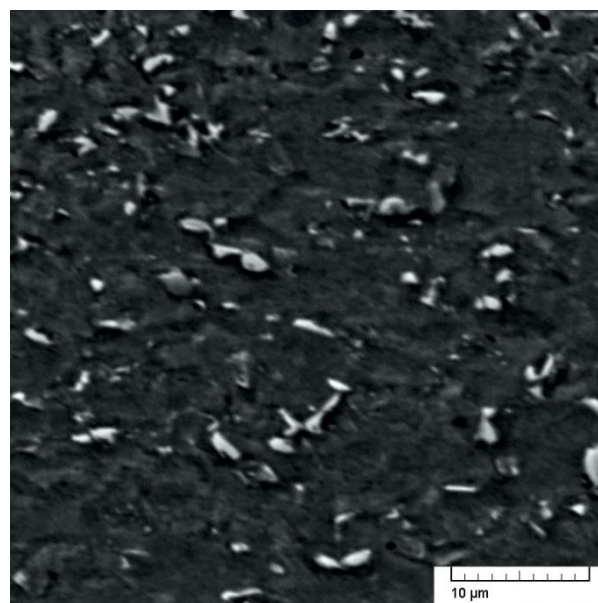


Figure 5. The initial structure of the 1.0939/HCT500X DP steel.

In the region of the heat-affected zone, close to the initial structure, laser exposure results in transient-layered and finely dispersed structures as a consequence of multiple heating and cooling cycles (region 2 in Figures 4 and 6a). At the selected processing parameters, the exposure time at high temperatures is short enough that the fibrous microstructure is no longer present in this area. The lighter regions in the immediate vicinity to the melting zone shown in Figure 6b (region 3 in Figure 4) represent small grains of ferrite, formed in a recrystallized structure.

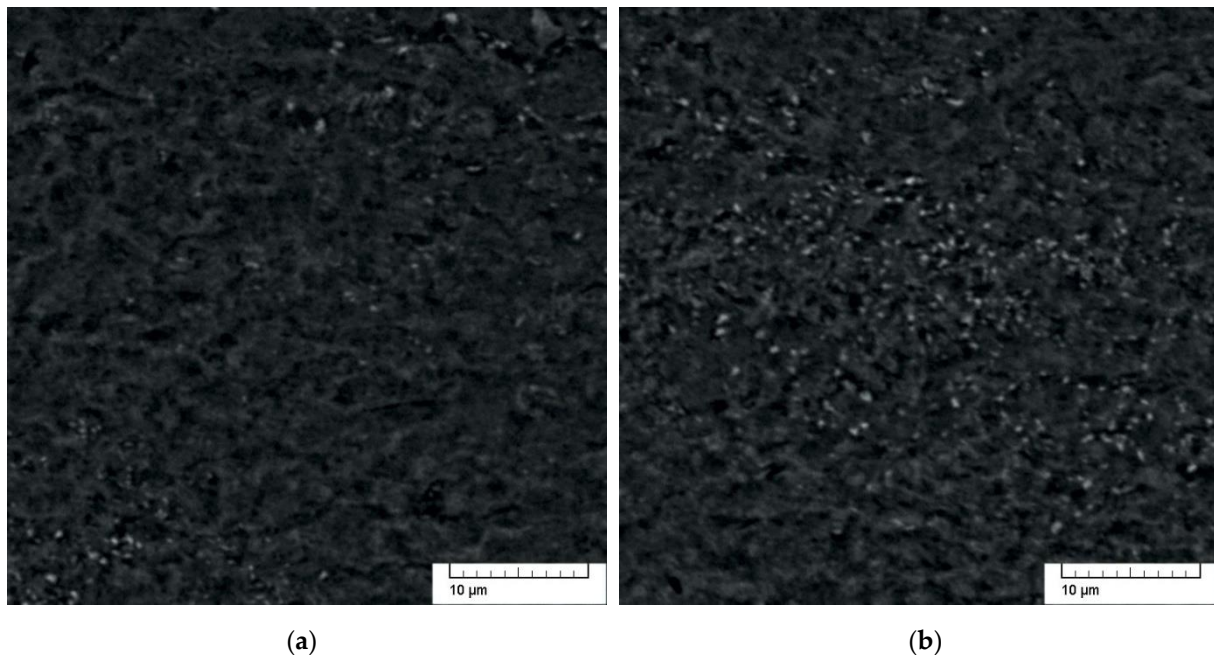


Figure 6. Images of the sample cross-section in the heat-affected zone: (a) close to the initial structure; (b) in the vicinity of the remelting zone.

When remelting regimes are used, the recrystallisation of the grain takes place, as a result of high-temperature heating. The characteristic initial structure of the steel disappears completely. After several cycles of melting and crystallisation, a finely dispersed structure of low-carbon martensite forms in the weld (region 4 in Figures 4 and 7a). It represents the result of multiple rapid remelting and solidification in the areas where the laser spots overlap. This structure is formed as a result of a relatively rapid cooling into the depth of the material. The lighter regions in Figure 7b (region 5 in Figure 4) also represent small grains of formed ferrite. The formation of the described metallic structures in the heat-affected and remelting zones during laser treatment can be explained by the difference in the parameters of the ongoing thermal cycles of heating and cooling. It is known that the value of cooling rate is related to the size of the cast zone and, thus, depends on the welding conditions. As the volume of the weld pool increases, the cooling rate in the remelted zone and the rate of crystallization decrease. Dendritic structures with developed interdendritic microheterogeneity are not observed in the melt pool.

MPM samples with a width of 16.2 mm were prepared for tensile testing of the welded joint. The results of the tensile tests performed on a Shimadzu AGS-100kNX testing machine at an applicable test speed of 1.5 mm/min showed a maximum tensile force of 3.78 kN and maximum elongation of about 0.6 mm. The typical stress–strain diagram for welded joints in the cross-section is presented in Figure 8. The strength of the welded area of the samples was 465 MPa, which constituted 80% of the measured ultimate strength of the base material 580 MPa.

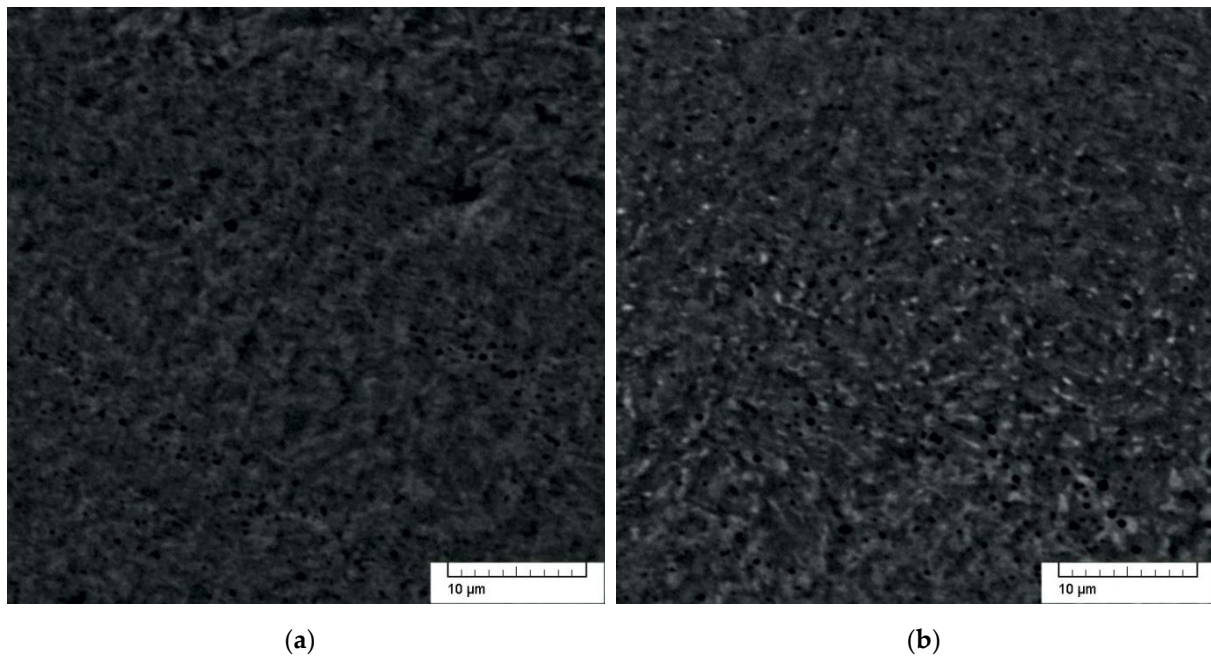


Figure 7. Images of the sample cross-section in the laser-processed area: (a) the fine-dispersed structure of low-carbon martensite in the remelting zone; (b) small grains of formed ferrite in the center of the weld.

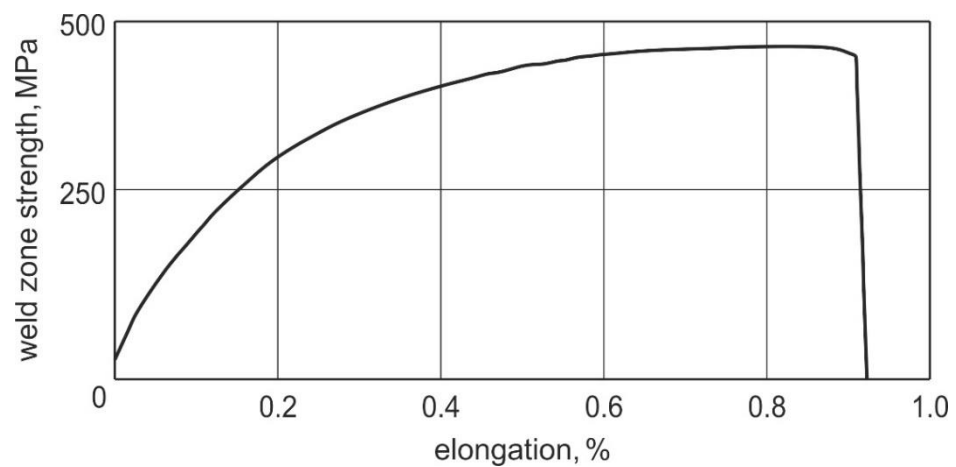


Figure 8. The stress–strain diagram of the welded zone of the samples.

The fractographic investigation of the fracture surface was carried out to evaluate the quality of the welded joint. This fracture surface was analyzed using an SEM and it was determined that its structure is homogeneous. The fracture surface is fibrous, with no metallic shine and without such defects as pores and non-metallic inclusions. Such a fine-grained fibrous fracture without shine indicates a sufficient plasticity and impact toughness of the metal material. An image of the fracture surface in the central area of the weld with clearly visible steel layers and a central polymer layer is shown in Figure 9. The thickness of the weld varied from 240 μm to 250 μm . Partial penetration welding of the steel plates allows one to avoid the degradation of the polymer core layer.

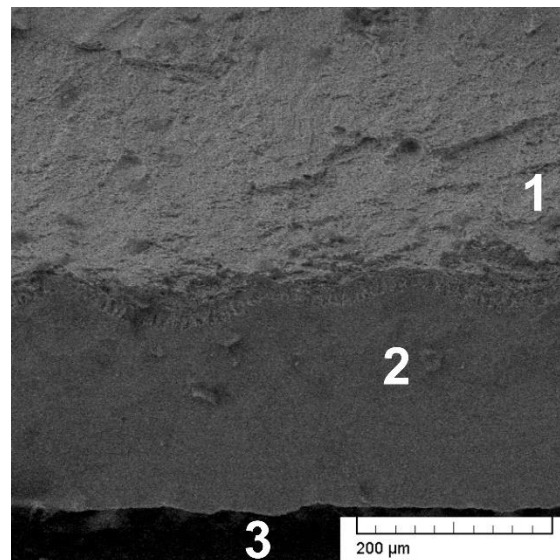


Figure 9. The surface of the fracture in the central area of the weld: 1—the zone of the fracture; 2—the non-fusion zone during laser welding; 3—the core polymer material.

Defocused laser beam welding is one of the easiest methods, allowing the redistribution of the laser energy density in order to improve the quality of the butt joint of metal–polymer sandwich composites. Further, by redistributing the beam energy density, the structure of the weld can be improved. However, there is non-uniformity in energy and power density across the laser spot, resulting in an unstable weld depth. At the same time, increased energy input can lead to increased residual stresses and deformations. Special optical systems must be used to increase the uniformity of energy and power density.

The formation of a weld by a laser beam in pulsed-periodic mode focused into a segment laser spot with a predetermined spatial distribution of energy and power density will provide an opportunity to obtain a welded joint with an increased area in the longitudinal section of each welded point. When exposed to such a heat source, the cross-sectional area of the weld will be minimal, thus, retaining the advantage of laser welding to produce welds that have a limited width accompanied by minimal deformation. The use of a diffractive free-form optical element [29,30] for beam shaping allows the creation of specified power and energy density profiles in the focal plane. This creates new methods for controlling the properties of the welded joint and opens up prospects for the laser welding of MPM sandwich panels.

4. Conclusions

As a result of the conducted investigations, the quality of butt joints of metal–polymer sandwich composites created by welding with redistribution of energy density of laser irradiation with an increasing laser spot diameter was improved. The task of increasing the joint strength of MPM samples made of DPK 30/50+ZE DP steel cover sheets with a thickness of 0.48 mm and thermoplastic polyolefin PP/PE as core material with a thickness of 0.6 mm was solved on condition of minimal degradation of the polymer core layer. Using a Rofin StarWeld Performance pulsed Nd:YAG laser, the two-sided welding of the MPM material was successfully carried out, resulting in partial penetration welds on each of the two sides of the material. An increase in the depth of melting zones to at least 50% of the thickness of the cover metal layers was achieved. Instead of previously obtained dendritic structures with developed interdendritic microheterogeneity in the heat-affected zone and the remelting zone, finely dispersed structures with better application prospects were created.

The experimental results showed that for certain values of energy and pulse duration, there is a certain diameter of the laser spot at which the penetration depth reaches a maximum. By gradually increasing the diameter of the laser spot, an increase in the penetration was observed only until the evaporation of the material ceased. Maximum penetration was achieved by laser welding in conduction mode, when the heat input density is not high enough to cause the evaporation of the material. When the pulse duration is in the range of a few milliseconds, the relatively small cross-sectional area of the melted zone can be attributed to the early reaching of intense evaporation due to the high power density in the beam. With increasing pulse duration, the maximum depth and diameter of the molten zone increase. However, once the pulse duration reaches two to three tens of milli-seconds, the energy losses due to thermal conduction increase to the extent that a further increase in duration no longer results in an increase in the size of the melt pool.

The parameters of the pulse-periodic mode of laser welding at which satisfactory results were obtained were identified as: pulse energy 32 J, pulse duration 8 ms and pulse frequency 1 Hz. The diameter of the laser spot on the material surface was 0.75 mm.

The structure of laser butt welds was investigated using a Neophot-30 polarised optical microscope and a VEGA\SB, Tescan scanning electron microscope. Metallographic studies of the samples showed that the welding area consisted of two zones: a melting zone and a heat-affected zone. Repeated heating and cooling cycles during laser exposure resulted in a transient-layered and fine-dispersed structure in the heat-affected zone. After multiple cycles of melting and crystallization, a fine-dispersed, low-carbon martensite structure was formed in the weld. Minor defects represented by micropores could be observed closer to the boundary of the metal remelting zone.

It should be noted that the important condition during the assembly of a butt joint is to avoid or maintain a minimum gap between the parts to be joined, and edge misalignment should be avoided. A significant improvement in welding conditions is achieved by machining the edges of the materials to be welded. At the same time, the required precision of the assembly is achieved.

Tensile tests performed on metal–polymer samples with a width of 16.2 mm revealed a maximum tensile force of 3.78 kN and maximum elongation of about 0.6 mm. As a result of the fracture surface analysis, it was determined that its structure is homogeneous, without pores and non-metallic inclusions. The obtained fine-grained fibrous fracture without shine indicates a sufficient plasticity and impact toughness in the metallic material. The strength of the base material was 580 MPa, while the strength of the welded area of the samples was registered as 465 MPa, which constitutes 80% of the base material strength.

The focusing of the laser beam into a segment with a predetermined distribution of energy and power density will provide an opportunity to obtain welded joints with an increased area in the longitudinal section of each welded point. The cross-sectional area of the weld will be minimal in this case, which is a characteristic feature of laser-welded joints and allows one to retain their advantages. By shaping the laser energy, diffractive freeform optical elements will allow one to achieve the specified profiles of power density and energy in the focal plane, thus, opening up new prospects for the laser welding of metal–polymer sandwich panels.

Author Contributions: Conceptualization, S.P.M. and H.P.; Methodology, S.P.M. and H.P.; Software, A.A.M., M.V.B. and S.O.; Validation, A.A.M.; Formal analysis, S.P.M. and A.A.M.; Investigation, A.A.M. and M.V.B.; Resources, S.P.M., H.P. and A.A.M.; Data curation, A.A.M. and S.O.; Writing—original draft preparation, S.P.M. and S.O.; Writing—review and editing, S.P.M. and H.P.; Visualization, A.A.M., M.V.B. and S.O.; Supervision, S.P.M.; Project administration, S.P.M. and H.P.; Funding acquisition, S.P.M. and H.P. All authors have read and agreed to the published version of the manuscript.

Funding: This research received no external funding.

Institutional Review Board Statement: Not applicable.

Informed Consent Statement: Not applicable.

Data Availability Statement: Data is contained within the article.

Conflicts of Interest: The authors declare no conflict of interest.

References

1. Vijaya Ramnath, B.; Alagarraja, K.; Elanchezhian, C. Review on sandwich composite and their applications. *Mater. Today Proc.* **2019**, *16*, 859–864. [[CrossRef](#)]
2. Seyed Jafari, P.; Hashemi, R.; Kazemi, F.; Pourmorad Kaleybar, S. An experimental investigation of mechanical properties, forming limit curves, and bending behavior of aluminum-polymer sandwich composites. *Mater. Res. Express* **2021**, *8*, 086516. [[CrossRef](#)]
3. Harhash, M.; Palkowski, H. Incremental sheet forming of steel/polymer/steel sandwich composites. *J. Mater. Res. Technol.* **2021**, *13*, 417–430. [[CrossRef](#)]
4. Palkowski, H.; Giese, P.; Wesling, V.; Lange, G.; Spieler, S.; Göllner, J. Neuartige Sandwichverbunde—Herstellung, Umformverhalten, Fügen und Korrosionsverhalten. *Mater. Werkst.* **2006**, *37*, 605–612. [[CrossRef](#)]
5. Gower, H.L.; Richardson, I.M.; Pieters, R.R.G.M. Pulsed laser welding of Steelite, a steel polypropylene laminate. *Sci. Technol. Weld Join.* **2006**, *11*, 593–599. [[CrossRef](#)]
6. Gower, H.L.; Pieters, R.R.G.M.; Richardson, I.M. Pulsed laser welding of metal-polymer sandwich materials using pulse shaping. *J. Laser Appl.* **2006**, *18*, 35–41. [[CrossRef](#)]
7. Salonitis, K.; Drougas, D.; Chryssoulouris, G. Finite element modeling of penetration laser welding of Sandwich materials. *Phys. Procedia* **2010**, *5*, 327–335. [[CrossRef](#)]
8. Salonitis, K.; Stavropoulos, P.; Fysikopoulos, A.; Chryssoulouris, G. CO₂ laser butt-welding of steel sandwich sheet composites. *Int. J. Adv. Manuf. Syst.* **2013**, *69*, 245–256. [[CrossRef](#)]
9. Buffa, G.; Campanella, D.; Forcellese, A.; Fratini, L.; Simoncini, M. Solid state joining of thin hybrid sandwiches made of steel and polymer: A feasibility study. *Procedia Manuf.* **2020**, *47*, 400–405. [[CrossRef](#)]
10. Murzin, S.P.; Palkowski, H.; Melnikov, A.A.; Blokhin, M.V. Laser welding of metal-polymer-metal sandwich panels. *Metals* **2022**, *12*, 256. [[CrossRef](#)]
11. Punzel, E.; Hugger, F.; Dinkelbach, T.; Bürger, A. Influence of power distribution on weld seam quality and geometry in laser beam welding of aluminum alloys. *Procedia CIRP* **2020**, *94*, 601–604. [[CrossRef](#)]
12. Möbus, M.; Woizeschke, P. Laser beam welding setup for the coaxial combination of two laser beams to vary the intensity distribution. *World Weld.* **2022**, *66*, 471–480. [[CrossRef](#)]
13. Mi, Y.; Mahade, S.; Sikström, F.; Choquet, I.; Joshi, S.; Ancona, A. Conduction mode laser welding with beam shaping using a deformable mirror. *Opt. Laser Technol.* **2022**, *148*, 107718. [[CrossRef](#)]
14. Noori Rahim Abadi, S.M.A.; Mi, Y.; Sikström, F.; Ancona, A.; Choquet, I. Effect of shaped laser beam profiles on melt flow dynamics in conduction mode welding. *Int. J. Therm. Sci.* **2021**, *166*, 106957. [[CrossRef](#)]
15. Sołtysiak, R.; Giętka, T.; Sołtysiak, A. The effect of laser welding power on the properties of the joint made of 1.4462 duplex stainless steel. *Adv. Mech. Eng.* **2018**, *10*, 1–12. [[CrossRef](#)]
16. Ayoola, W.A.; Suder, W.J.; Williams, S.W. Effect of beam shape and spatial energy distribution on weld bead geometry in conduction welding. *Opt. Laser Technol.* **2019**, *117*, 280–287. [[CrossRef](#)]
17. Kuryntsev, S.V.; Gilmudtinov, A.K.; Shiganov, I.N. Welding with a defocused laser beam. *Weld. Int.* **2017**, *31*, 151–156. [[CrossRef](#)]
18. Kuryntsev, S.; Kolesnikov, D.; Vulpe, M. Investigation of the effect of welding heat input and focal distance of laser beam on penetration depth and dynamics of welding pool using a high-speed video camera. *Mater. Sci. Forum* **2020**, *989*, 721–732. [[CrossRef](#)]
19. Sundqvist, J.; Kaplan, A.F.H.; Shachaf, L.; Brodsky, A.; Kong, C.; Blackburn, J.; Assuncao, E.; Quintino, L. Numerical optimization approaches of single-pulse conduction laser welding by beam shape tailoring. *Opt. Lasers Eng.* **2016**, *79*, 48–54. [[CrossRef](#)]
20. Kong, C.Y.; Bolut, M.; Sundqvist, J.; Kaplan, A.F.H.; Assunção, E.; Quintino, L.; Blackburn, J. Single-pulse conduction limited laser welding using a diffractive optical element. *Phys. Procedia* **2016**, *83*, 1217–1222. [[CrossRef](#)]
21. Kumar, N.; Mukherjee, M.; Bandyopadhyay, A. Study on laser welding of austenitic stainless steel by varying incident angle of pulsed laser beam. *Opt. Laser Technol.* **2017**, *94*, 296–309. [[CrossRef](#)]
22. Chludzinski, M.; dos Santos, R.E.; Churiaque, C.; Fernández-Vidal, S.R.; Ortega-Iguña, M.; Sánchez-Amaya, J.M. Pulsed laser butt welding of AISI 1005 steel thin plates. *Opt. Laser Technol.* **2021**, *134*, 106583. [[CrossRef](#)]
23. Xue, X.; Pereira, A.B.; Amorim, J.; Liao, J. Effects of pulsed Nd: YAG laser welding parameters on penetration and microstructure characterization of a DP1000 steel butt joint. *Metals* **2017**, *7*, 292. [[CrossRef](#)]
24. Murzin, S.P.; Kazanskiy, N.L.; Stiglbrunner, C. Analysis of the advantages of laser processing of aerospace materials using diffractive optics. *Metals* **2021**, *11*, 963. [[CrossRef](#)]
25. Murzin, S.P.; Liedl, G. Laser welding of dissimilar metallic materials with use of diffractive optical elements. *Computer Optics* **2017**, *41*, 848–855. [[CrossRef](#)]
26. EN 10346:2009; Continuously Hot-Dip Coated Steel Flat Products—Technical Delivery Conditions. European Committee for Standardization: Brussels, Belgium, 2009.

27. Richter, J.; Kuhtz, M.; Hornig, A.; Harhash, M.; Palkowski, H.; Gude, M. A mixed numerical-experimental method to characterize metal-polymer interfaces for crash applications. *Metals* **2021**, *11*, 818. [[CrossRef](#)]
28. Harhash, M.; Kuhtz, M.; Richter, J.; Hornig, A.; Gude, M.; Palkowski, H. Influence of adhesion properties on the crash behavior of steel/polymer/steel sandwich crashboxes: An experimental study. *Metals* **2021**, *11*, 1400. [[CrossRef](#)]
29. Murzin, S.P.; Kazanskiy, N.L.; Stiglbrunner, C. Development of technologies of laser material processing with use of diffractive optics. In Proceedings of the ITNT 2021—7th IEEE International Conference on Information Technology and Nanotechnology, Samara, Russia, 20–24 September 2021.
30. Murzin, S.P.; Blokhin, M.V. Selective modification of dual phase steel DP 1000 by laser action using diffractive optical element. *Comput. Opt.* **2019**, *43*, 773–779. [[CrossRef](#)]